A Simple Melt Impregnation Method to Synthesize Ordered Mesoporous Carbon and Carbon Nanofiber Bundles with Graphitized Structure from Pitches

Haifeng Yang, Yan Yan, Ying Liu, Fuqiang Zhang, Renyuan Zhang, Yan Meng, Mei Li,[†] Songhai Xie, Bo Tu, and Dongyuan Zhao*

Department of Chemistry and Shanghai Key Laboratory of Molecular Catalysis and Innovative Materials, Fudan University, Shanghai 200433, P. R. China, and Department of Material Science and Technology, Northwest Polytechnique University, Xi'an, Shanxi, 710072, P. R. China

Received: July 9, 2004; In Final Form: September 1, 2004

In this paper, we report a simple melt impregnation method by using cheap mesophase pitches (MPs) as carbon precursors to prepare ordered mesoporous carbon with ordered graphitized pore walls at low temperature. This facile procedure includes melting MPs at 140 °C and impregnation of the melt into hexagonal or bicontinuous cubic mesoporous silica templates. After the removal of silica templates by HF solution, ordered mesoporous carbon materials with replica structures of 2-D hexagonal *p*6*mm* or cubic $Ia\bar{3}d$ symmetry were derived. The pore walls of the hexagonal mesoporous carbon products are composed of graphitized domains with the (002) crystallographic plane of the graphite perpendicular to the long axis of the carbon nanorods. Theoretical computations show that negatively charged O atoms of Si−OH and Si−O−Si from the surface of mesoporous silica channels can interact with the positive charged H atoms of the MPs, which makes the stacking units incorporate into the pores with the (002) plane vertical to the channels, and finally the oriented periodicity of the graphite domains is formed. N_2 sorption measurements show that the materials possess no micropores. For the bicontinuous cubic mesoporous carbon, HRTEM images show that the material is a true replica framework of $Ia\bar{3}d$ symmetry. The graphitized structure of the pore walls seems to have an orientation related to the bicontinuous pore structure, which could not be simply defined based on current TEM results. Graphitized carbon nanofiber bundles with a uniform diameter of about 7 nm were obtained by using Fe_2O_3 nanoparticle doped mesoporous silica as a template. A spiral graphite structure was observed for the materials. Cyclic voltammetry measurements show low charge/discharge currents for the graphitized materials compared to the amorphous mesoporous carbon, further confirming the anisotropic character of the graphitized mesoporous carbons. The method can be widely applied to the hard-templating synthesis of graphitized carbon nanostructures and other doped carbon nanomaterials.

Introduction

Ordered mesoporous carbons, designated as CMK materials, have been intensively studied because of their potential applications in catalysis, sorption, electronics, sensors, and so on.[1−5] The preparation of these kind of materials follows a typical nanocasting procedure. To be specific, sucrose can be used as a carbon precursor and completely incorporated into the channels of mesoporous silica templates by a controllable two-step impregnation process. After carbonization of the precursor and dissolution of the templates, the obtained mesoporous carbons well maintain the macroscopical morphology and ordered mesostructure of the silica templates, which can be considered as ordered nanorod (or nanotube) arrays with amorphous carbon structure.[5−7] From the viewpoint of pore structures, those carbon materials are replica frameworks of the silica templates, but an exception is the $Ia\bar{3}d$ structure. Because of the structure transformation of the two sets of separated frameworks, mesoporous materials with lower $I4_132$ symmetry are usually derived by using mesoporous silica MCM-48 as a template.[1,8]

It is well-known that the electrical and sorption properties of carbon materials are closely related to their graphite nature. Recently, detailed structural characterization by nitrogen sorption has shown that, upon heating treatment at 1600 °C, information on the graphitized order on the outer surface of the mesopore walls of CMK-3 and CMK-1 is detected.[9,10] More recently, a new pathway has been reported by Ryoo and co-workers.[11] They put Al incorporated SBA-15 and acenaphthene into a special alloy autoclave under Ar atmosphere and heated the autoclave at 750 °C for 2 h. After the autoclave was cooled to room temperature the products were heated to 900 °C under vacuum in a fused quartz. By using such a complicated method, Ryoo and co-workers have successfully obtained ordered mesoporous carbons with graphitized structure after removing the silica templates. Moreover, the method was reported to be versatile for silica templates of different mesostructures, but detailed characterization for bicontinuous cubic structure has not been reported. Till now, mesoporous carbon with completely graphitized structure remains an interesting topic for researchers and facile synthetic routes for those materials are still much expected.

Mesophase pitches (MPs), synthetic pitches derived from polyaromatic systems, are a type of cheap carbon sources and are generally considered as polydomain liquid crystallines constructed by well-stacking layers of carbon rings, which makes

* Address correspondence to this author at Fudan University. E-mail: dyzhao@fudan.edu.cn.
[†] Northwest Polytechnique University.

10.1021/jp046948n CCC: $27.50
Published on Web 10/20/2004

SCHEME 1: The Simple Melt Impregnation Procedure for Preparation of Ordered Mesoporous Carbon Materials and Carbon Nanofiber Bundles with Graphitized Structure

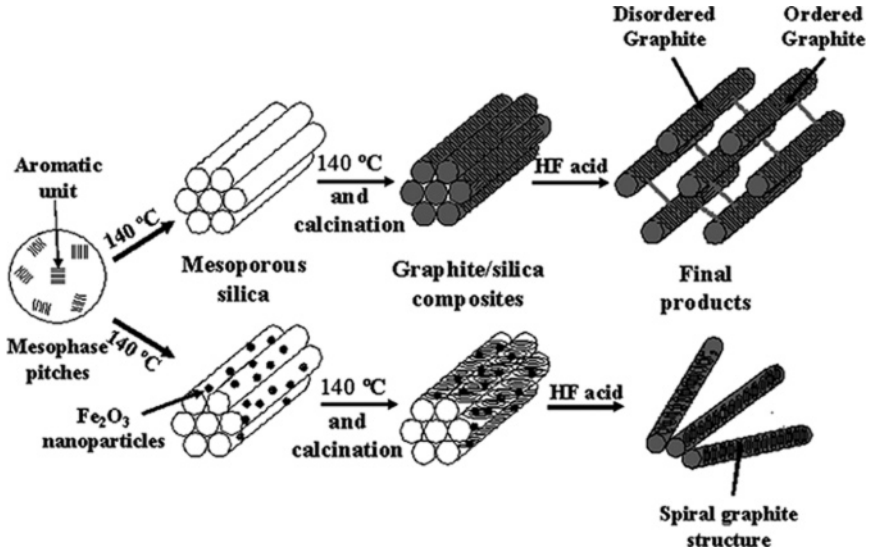

the carbon obtained from the MPs highly graphitizable compared to those from other carbon precursors.[12] Besides, MPs are predominantly anisotropic, featured with a relatively low viscosity and a high coke yield (beyond 80 wt %). All these special properties are extremely beneficial to the preparation of carbon materials with high thermal and electrical conductivity. Therefore, MPs are widely used as carbon precursors in preparing carbon-reinforced composites.[13] Jaroniec and co-workers have reported the synthesis of disordered large-pore mesoporous carbon with MPs through a colloidal templating method; however, only the fluidity at high temperature of the precursor is utilized in the research.[14] By using porous materials as hard templates, carbon nanostructures can also be obtained from MPs; however, no specific characterization and mechanism studies are provided.[15]

In this paper, we report a one-step melt impregnation method to prepare ordered mesoporous carbons with ordered graphitized structure at low temperature by using MPs as carbon precursors. This very facile preparation procedure is just simply impregnating the melt mesophase pitches into mesoporous silica templates at 140 °C. After the removal of the silica template by HF solution, ordered replica mesoporous carbon products with two-dimensional (2-D) hexagonal (*p*6*mm*) or 3-D bicontinuous cubic ($Ia\bar{3}d$) structures can successfully be obtained. High-resolution transmission electron microscopy (HRTEM) images show that the hexagonal mesoporous carbons are composed of graphitized domains with a (002) crystallographic plane of the graphite perpendicular to the long axis of the carbon nanorods. Theoretical molecular simulations reveal this orientation can be attributed to the noncovalent interaction between negative charged O atoms of the silica templates and MPs. Furthermore, 3-D bicontinuous mesoporous carbon products are true replica frameworks of $Ia\bar{3}d$ symmetry with complicated graphitized structure orientation. This facile method can also be used to prepare bundles of graphitized carbon nanofibers with the uniform diameter of 7 nm by using Fe_2O_3 nanoparticle doped mesoporous silica as a hard template. A spiral graphitized structure is observed for the carbon nanofiber bundles. Compared with the amorphous mesoporous carbon, the graphitized materials are proved to be anisotropic and present low surface areas and pore volumes.

Experimental Section

The mesoporous graphitized carbons and carbon nanofiber bundles were synthesized through a simple one-step melt impregnation procedure by using MPs as carbon precursors and mesoporous silica materials as templates. As shown in Scheme 1, the process mainly included melting the pitch powders at a low temperature (140 °C) and impregnating the melt pitches into the mesoporous silica powders with stirring. After the carbonization, the silica templates were dissolved with HF acid.

Preparation of Mesoporous Silica Templates. 2-D hexagonally ordered mesoporous silica materials SBA-15 were prepared by using block copolymer P123 (Pluronic 123, EO_{20}-$PO_{70}EO_{20}$) as a structure-directing agent under acidic condition at 40 °C according to the previous report.[16] 3-D bicontinuous cubic mesoporous silica materials with $Ia\bar{3}d$ symmetry were prepared by using P123 as a structure-directing agent and butanol as organic assisted agent, which was improved similarly to the pathway reported by Ryoo and co-workers.[17] As for the preparation of graphitized carbon nanofiber bundles, ordered hexagonal mesoporous silica materials doped with Fe_2O_3 nanoparticles in the channels were used as the templates, and a previously reported one-step synthetic pathway was employed[18] except that $Fe(NO_3)_3 \cdot 6H_2O$ was used as a metal precursor. The mass ratio of Fe:Si was 1:5 in the initial reaction composites. The samples derived were 2-D hexagonal mesoporous silica with Fe_2O_3 nanoparticles in the channels and the nanoparticles were around 5 nm in dimension based on XRD and TEM observations.

Preparation of Mesoporous Graphitized Carbons. For a typical synthesis, 1.05 g of mesophase pitches (prepared with the traditional catalytic pathway,[12] softening temperature 104 °C, $\rho = 1.3$ g cm^{-3}) was heated at 140 °C in a ceramic crucible with stirring for 0.5 h until a highly flexible fluidic black melt was formed. One gram of hexagonal or bicontinuous cubic mesoporous silica material was added to the melt step by step during stirring, finally yielding dark brown powders. The carbon/silica mesostructured composites were calcined at 800 °C for 6 h under N_2 atmosphere for the carbonation. To remove silica templates, the solid samples were dissolved in HF aqueous solution (10 wt %) and stirred for 24 h. After filtration, black powders were rinsed with distilled water three times and dried

in the ambient condition. The yield of the carbon materials was higher than 65% calculated from the amount of MPs used.

Preparation of Graphitized Carbon Nanofiber Bundles. The procedure described above was followed for the synthesis, but the template was replaced with the iron oxide nanoparticle doped mesoporous silica and the mass ratio of MPs to template silica was 1.0:1.1.

Preparation of Ordered Mesoporous Carbon CMK-3. The material was synthesized with the method reported by Ryoo and co-workers by using ordered mesoporous silica SBA-15 as a template and sucrose as a carbon precursor.[19] A successive two-step impregnation procedure and high-temperature calcination at 900 °C under N_2 atmosphere were employed. The silica template was dissolved by HF acid.

Theoretical Computation Details. The interaction between the silica walls and the graphene layers can be understood with thermodynamic calculations. The preliminary computation was carried out with simple theoretical models of a single Si, O, and H unit as the silica wall and two pyrene molecules as graphene layers. As for such multiobject systems with a heavy atom (Si), the semiemperical AM1 method was selected to process the full geometry optimization. After the frequency calculation, the final structures (shown later in Scheme 3) had no negative frequencies and were confirmed to be the most stable ones. The dihedral angle parameters could be obtained from the geometry computation for discussing the mechanism. All the theoretical computations were performed with the Gaussion 98 program package on a Dell Dimension computer at the laboratory of molecular catalysis and innovative materials, Fudan University

Electrochemical Measurements. Electrochemical measurements were preformed with a CHI 1030 electrochemical workstation (CHI), using a three-electrode system, with the mesoporous carbon products as the working electrode, a platinum wire as the counter electrode, and a saturated calomel electrode (SCE) as the reference in a thermostat. The derived graphitized mesoporous carbon products with different pore structures and graphitized carbon nanofiber bundles as well as CMK-3 for comparison were used to prepare the working electrode. The carbon powders respectively were dispersed in 1% Nafion monomer solution (diluted in PBS, phosphate buffer solution) with the concentration of 0.5 mg/mL and sonicated for 10 min. A 10-μL sample of the mixture was dipped onto a glassy carbon electrode (polished with Al_2O_3 paste and washed ultrasonically in double-distilled water) and solidified for 4 h at 25 °C. Cyclic voltammetry (CV) was conducted in 1 M H_2SO_4 solution at 25 °C with a scan rate of 100 mV/S, using the obtained thin film glassy carbon electrode as a working electrode.

Characterization. Powder X-ray diffraction (XRD) patterns were recorded with a Bruker D4 powder X-ray diffractometer, using Cu Kα radiation. Transmission electron microscopy (TEM) images were taken with a JEOL JEM2011 electron microscope operating at 200 kV. For TEM measurements, the samples were prepared by dispersing the powder products as a slurry in ethanol, after which they were dispersed and dried on a holey carbon film on a Cu grid. The nitrogen adsorption−desorption isotherms were measured with a Quantachrome Autosorb-1 analyzer at 77 K. Before the measurement, the samples were degassed under vacuum at 180 °C for 5 h. The Brunauer−Emmett−Teller (BET) method was utilized to calculate the surface areas. The pore volume and pore size distributions were derived from the adsorption branches of the isotherms with use of the Barrett−Joyner−Halanda (BJH) method. Raman spectra (RS) were obtained with a Dilor LabRam-1B microscopic Raman spectrum, using the He−Ne laser with the excitation wavelength of 632.8 nm.

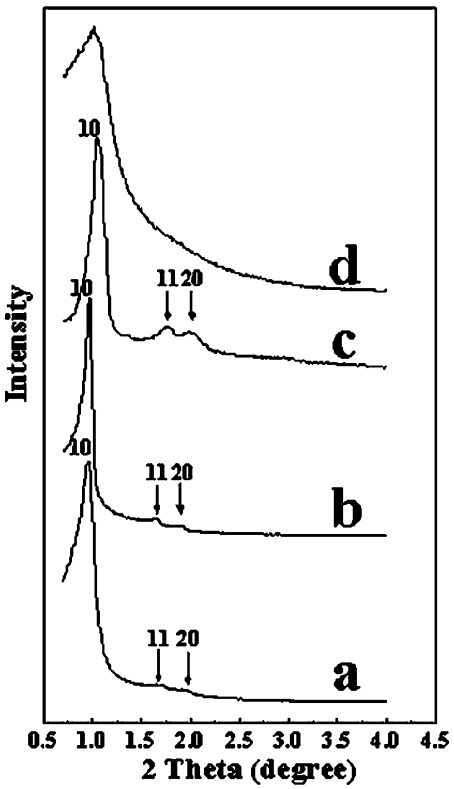

Figure 1. Small-angle XRD patterns of (a) ordered hexagonal mesoporous graphitized carbons with *p*6*mm* symmetry prepared from the simple melt impregnation method by using mesophase pitches as a carbon source, (b) calcined mesoporous silica SBA-15, (c) calcined hexagonal mesoporous silica doped with Fe_2O_3 nanoparticles, and (d) graphitized carbon nanofiber bundles prepared from the melt impregnation method by using Fe_2O_3 nanoparticle doped mesoporous silica as a template.

Results

1. Hexagonal Mesoporous Graphitized Carbon With *p*6*mm* Symmetry. Ordered graphitized mesoporous carbon with *p*6*mm* symmetry can be synthesized via the simple melt impregnation method by using MPs as carbon precursors and SAB-15 as a template. The small-angle XRD pattern (Figure 1a) of the carbon products shows well-resolved diffraction peaks, indicating that ordered mesostructure is maintained after the removal of the mesoporous silica template. The three diffraction peaks can be indexed to (10), (11), and (20) diffraction of ordered 2-D hexagonal mesostructure with a space group of *p*6*mm*, which is similar to that for CMK-3, a carbon replica of SBA-15.[19] Compared with the XRD pattern of the mesoporous silica template SBA-15 (Figure 1b), the (10) peak of the carbon material has a slight shift from 2θ of 0.91° to 0.95°, implying a little structural shrinkage because of the high-temperature calcined process.

The XRD pattern (Figure 2a) at the wide-angle range (20−60°) for the 2-D hexagonal mesoporous carbon products with *p*6*mm* symmetry shows two intensive diffraction peaks which can be indexed to (002) and (100) diffraction for typical graphite carbons. The *d* spacing of the (002) plane is 0.35 nm and a little bigger than the value (0.343 nm) of graphitized carbons derived up to 2800 °C, suggesting that the materials are still not perfectly graphitized with the low calcination temperature

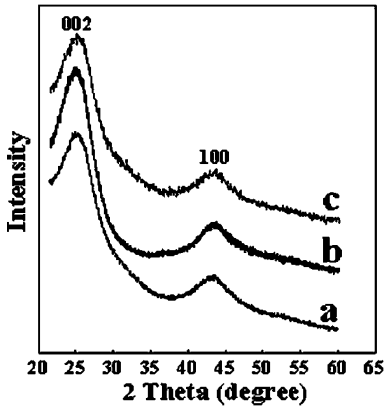

Figure 2. Wide-angle XRD patterns of ordered mesoporous graphitized carbon products with (a) 2-D hexagonal *p*6*mm* and (b) bicontinuous cubic $Ia\bar{3}d$ symmetry and (c) graphitized carbon nanofiber bundles prepared by using Fe_2O_3 nanoparticle doped mesoporous silica as a template.

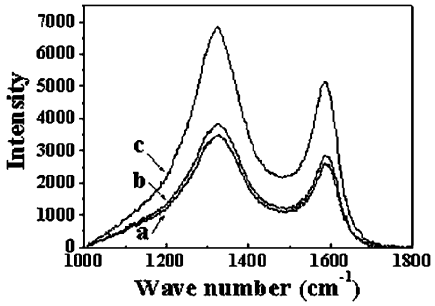

Figure 3. Raman spectra of ordered mesoporous graphitized carbon products with (a) 2-D hexagonal *p*6*mm* and (b) bicontinuous cubic $Ia\bar{3}d$ symmetry and (c) graphitized carbon nanofiber bundles.

(800 °C).[12] Raman spectroscopy (RS) is considered to be the a solid method for studying carbon phase and the vibration at 1580 cm^{-1} (G-band) due to the interplane sp^2 C−C stretching is the characteristic feature of ordered graphite carbon.[13] A strong band at 1576 cm^{-1} can be observed (Figure 3a) for the mesoporous carbon products prepared from the simple melt impregnation method, revealing a well-defined graphitized structure. Another band at around 1340 cm^{-1} (D-band) caused by the defects within the carbon microtextures with regard to the ideal graphitized structure can also be observed, which is in accord with the larger *d* spacing values of the (002) plane from XRD results.

A more detailed structural study was carried out with TEM characterization for the mesoporous carbon prepared by using the low-temperature melt impregnation method and MPs as carbon precursors. As shown in Figure 4, large domains with ordered strut-like (Figure 4a) and hexagonal (Figure 4b) carbon arrays are observed for the graphitized mesoporous carbon materials templated from hexagonal mesoporous silica SBA-15. The unit cell parameter (*a*) of the sample is calculated to be 10.9 nm, in good agreement with the value determined from the XRD data. HRTEM images along the [001] direction (Figure 4c,d) further confirm that the pore walls of the 2-D hexagonal mesoporous carbon products are constructed with the domains of graphitized carbon. The *d* spacing of the observed lattice planes is ca. 0.35 nm, in accord with the *d*(002) spacing calculated from XRD results. The corresponding selected area electron diffraction (SAED) pattern (Figure 4e) shows an obvious periodicity of the crystalline pore walls caused by (002) diffraction and further proves that the orientation of the graphite lattices is perpendicular to the long axis (*c* axis) of the

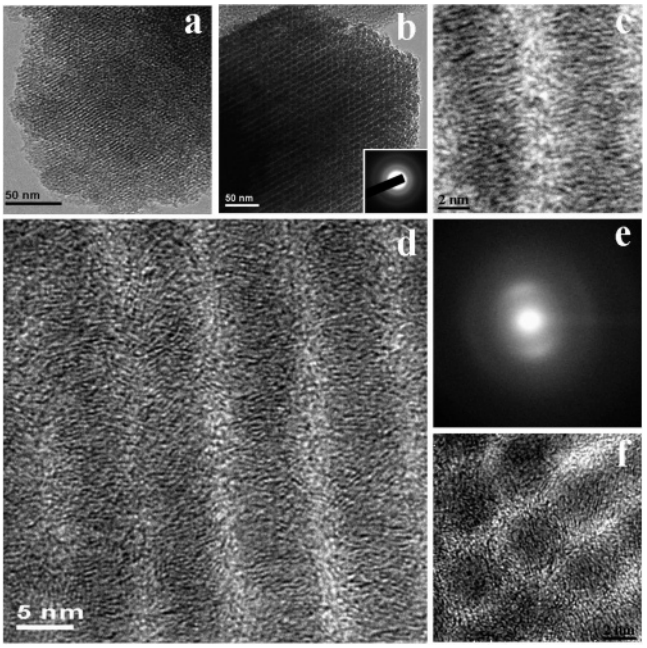

Figure 4. TEM images of ordered mesoporous graphitized carbon materials with 2-D hexagonal *p*6*mm* symmetry along the (a) [001] and (b) [100] directions; HRTEM images of mesoporous graphite carbon materials along (c and d) [001] and (f) [100] directions, and corresponding SAED patterns of the observed domains along (e) [001] and (inset of b) [100] directions.

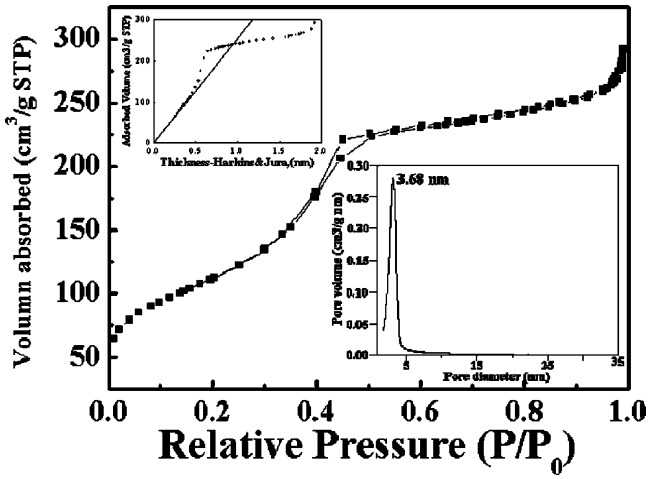

Figure 5. Nitrogen adsorption/desorption isotherm plots, pore size distribution curve (inset), and *t*-plot curves of ordered 2-D hexagonal mesoporous graphitized carbon prepared from the simple melt impregnation method by using SBA-15 as a template.

mesoporous carbon rods. Graphitized structure can also be found at some tiny domains in the HRTEM image along the [110] direction (Figure 4f), owing to the occasionally distorted graphite layers. The corresponding SAED pattern (Figure 4b, inset) with a feature of polycrystalline materials indicates the irregular orientation in the [110] direction, which is in accord with the HRTEM and RS results.

The graphitized mesoporous carbon products with 2-D hexagonal *p*6*mm* symmetry obtained from the facile low-temperature melt impregnation method by using MPs as carbon precursors yield a representative type IV isotherm of N_2 sorption with H_1 hysteresis loops at 77 K (Figure 5). A well-defined step occurs approximately at $p/p_0 = 0.30-0.70$, which is associated with the filling of the mesopores due to capillary condensation. Narrow pore-size distribution (right insets of

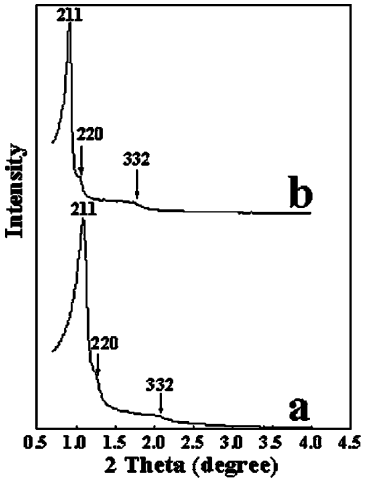

Figure 6. Small-angle XRD patterns of (a) ordered bicontinuous cubic *Ia*$\bar{3}$*d* mesoporous graphitized carbon prepared from the simple melt impregnation method by using mesophase pitches as a carbon source and (b) calcined mesoporous silica with *Ia*$\bar{3}$*d* symmetry prepared by using block copolymer P123 as a structure-directing agent and butanol as organic assisted agent under acidic condition.

Figure 5) is calculated from the adsorption branch based on BJH model, indicating that the carbon materials have a very uniform mesopore structure. For the hexagonal mesoporous carbon products, the pore size, BET surface area, and pore volume are 3.68 nm, 390 m^2/g, and 0.43 cm^3/g, respectively. The surface areas and pore volumes of the samples are much lower than the normal amorphous mesoporous carbons, such as CMK-3 with the same pore structures (for CMK-3, the surface area and pore volume are 1500 m^2/g and 1.3 cm^3/g, respectively[2]). The reason may be attributed to the graphitized crystalline nature of the carbon materials. As reported previously, the micropores of the amorphous mesoporous carbons contributed significantly to the surface area and pore volume;[20] however, the graphitized mesoporous carbon reported here is composed of graphitized carbon walls. Different from the randomly packed tiny domains of amorphous carbon to achieve micropores, the material contains well-stacking graphene layers, which are more densified than those amorphous mesoporous carbons, and no micropores can be formed in such a structure. As calculated from the *t*-plot curves (left insets of Figure 5), the materials possess no adsorption of micropores, suggesting the surface area and pore volume both arise from mesopores only. This result is in agreement with the special graphitized structure of the materials.

2. Bicontinuous Mesoporous Graphite Carbon with *Ia*$\bar{3}$*d* Symmetry. This simple melt impregnation method can also be applied to the preparation of ordered mesoporous graphitized carbon with *Ia*$\bar{3}$*d* symmetry by using large pore bicontinuous cubic mesoporous silica as a template. As shown in Figure 6a, three intensive diffraction peaks can be observed in the small-angle XRD pattern of the mesoporous carbon products, which is similar to the mesoporous silica templates (Figure 6b). The diffraction peaks can be indexed to (211), (220), and (332) reflections of ordered cubic mesostructure for space group *Ia*$\bar{3}$*d*. But the (332) peak is slightly broadened due to the overlap of the (400), (420), and (422) peaks. The diffraction peak of (110) for the mesoporous carbon of $I4_132$ symmetry templated by MCM-48 is not observed,[1] confirming the pure *Ia*$\bar{3}$*d* symmetry of the mesoporous carbon products prepared from this simple melt impregnation method. Different from previous reports, the mesoporous carbon derived here is believed to be the true replica structure of mesoporous silica with *Ia*$\bar{3}$*d* symmetry. Similar to

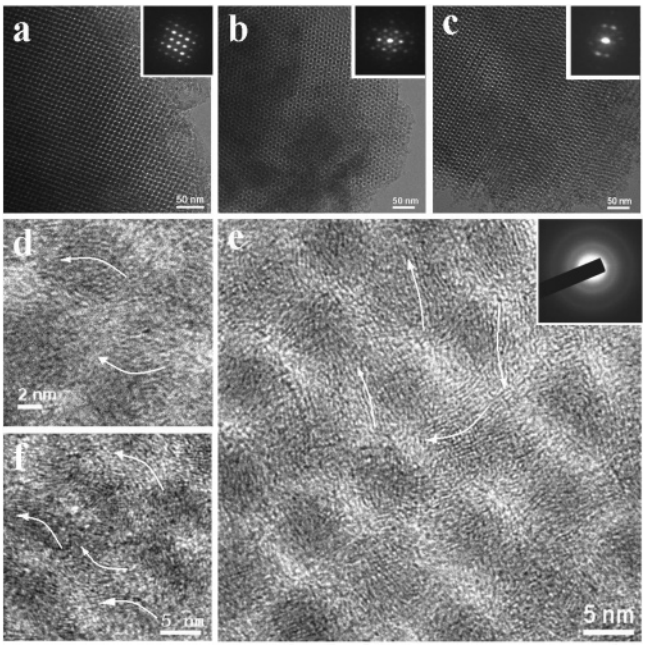

Figure 7. TEM images of ordered mesoporous graphitized carbon with bicontinuous cubic *Ia*$\bar{3}$*d* symmetry along the (a) [110], (d) [111], and (c) [311] directions; the insets of panels a, b, and c are the corresponding SAED patterns; HRTEM images of the sample along the (d) [110], (e) [111], and (f) [311] directions. The inset of panel e is the corresponding SAED pattern of the observed area. The white arrows are the observed orientation of the graphitized lattices.

the above results regarding the hexagonal mesoporous carbons, wide-angle XRD and RS (Figure 2b and 3b, respectively) prove that the bicontinuous cubic mesoporous carbon products with *Ia*$\bar{3}$*d* symmetry prepared by the facile melt impregnation method are also composed of the graphitized carbon structure.

TEM images from three characteristic directions along [110], [111], and [311] (Figure 7a−c) clearly show the bicontinuous cubic mesostructure *Ia*$\bar{3}$*d* of the graphitized carbon materials prepared from the melt impregnation method by using MPs as carbon precursors. The corresponding SAED patterns (insets of Figure 5a−c) further confirm the *Ia*$\bar{3}$*d* symmetry of the samples, suggesting the true carbon replica structure of the silica templates. The structural separation of the two sets of carbon frameworks has not been found for all the domains, which is in good agreement with the XRD results. Calculated from Figure 5b, the unit cell parameter (*a*) of the mesoporous carbon samples is 19.8 nm, which is in agreement with the XRD results. Lamellar graphitized structure can also be observed from the HRTEM images along the [110], [111], and [311] directions (Figure 7d−f). The lattice orientation seems to be related to the bicontinuous cubic mesostructure (Figure 7d−f). But due to the complexity of the pore structure, we could not define the relationship between the two scaled periodicities simply based on current TEM results.

A type IV N_2 sorption isotherm with an H_1 hysteresis loop at 77 K is also obtained for the bicontinuous mesoporous graphitized carbon with *Ia*$\bar{3}$*d* symmetry prepared from the melt impregnation by using MPs as carbon precursors (Figure 8). Notably, the hysteresis loop of the isotherm is extended to the low-pressure region around $P_0/P = 0.1-0.3$, which is quite special for mesoporous carbons. The reason may be attributed to the asymmetric pore size. The thicknesses of the pore walls of the mesoporous silica with *Ia*$\bar{3}$*d* symmetry are not identical everywhere due to the fascinating bicontinuous mesopores. Therefore, the pore size of the replica structure will also be

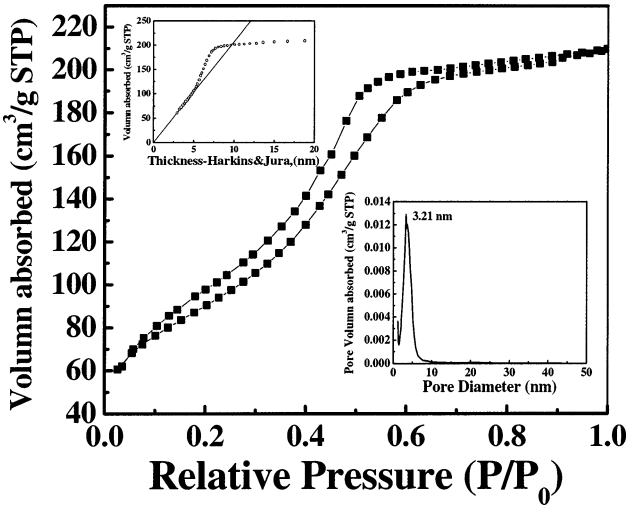

Figure 8. Nitrogen adsorption/desorption isotherm plots, pore size distribution curve (inset), and *t*-plot curves of ordered mesoporous graphitized carbon with $Ia\bar{3}d$ symmetry prepared from the simple melt impregnation method by using mesophase pitch as a carbon source.

asymmetric, and cause the large hysteresis loops, further revealing the true $Ia\bar{3}d$ replica structure of the sample here. The pore size, BET surface area, and pore volume are 3.21 nm, 330 m^2/g, and 0.32 cm^3/g, respectively. Similar to the hexagonal mesoporous graphitized carbons, the surface area and pore volume of the samples are much lower compared to the normal amorphous mesoporous carbons, such as CMK-4 with the same mesopore structures. The fact is that because of the lack of micropores, which give indirect testimony that the graphitized lattice of the mesoporous carbon has a certain orientation related to the $Ia\bar{3}d$ symmetry, the surface area for disordered graphitized growth of the pore walls would be higher than that for the above hexagonal mesoporous graphitized carbon products.

3. Graphitized Carbon Nanofiber Bundles. Besides the variation of the mesostructures, the orientation of the graphite crystallographic plane is also expected to be different. As reported before, Fe_2O_3 is an effective catalyst for graphene layer growth, namely the most important step of the graphitization process.[21] Therefore, hexagonal mesoporous silica materials doped with Fe_2O_3 nanoparticles were also used as templates to achieve larger graphitized layer growth in the mesopores and may possibly change the crystallographic orientation of the carbon replica materials.

By using the low-temperature melt impregnation method, graphitized carbon nanofiber bundles can be obtained. Compared to the mesoporous graphitized carbons, only one relatively broad peak is observed for the small-angle XRD pattern (Figure 1d) of the carbon samples templated by Fe_2O_3 nanoparticle doped mesoporous silica, implying partially ordered mesostructures. The first diffraction peak of the sample is shifted to a higher angle ($2\theta = 1.03°$) for a smaller $d(100)$ spacing value compared with that for mesoporous silica templates (Figure 1c, $2\theta = 0.98°$), implying that, after dissolving the silica framework, the carbon replica lost the ordered mesostructure due to the absence of the pillars between carbon nanorods. On the basis of chemical analysis data, detectable amounts of iron oxides cannot be observed on the final carbon products, suggesting that during the removal of the silica templates by using HF, Fe_2O_3 nanoparticles can also be removed. Wide-angle XRD results of the sample (Figure 2c) show a typical pattern for the graphitized carbon structure. But comparing the RS results (Figure 3), the G-band of the graphitized carbon nanofiber bundles is obviously stronger and narrower than that of the mesoporous graphitized

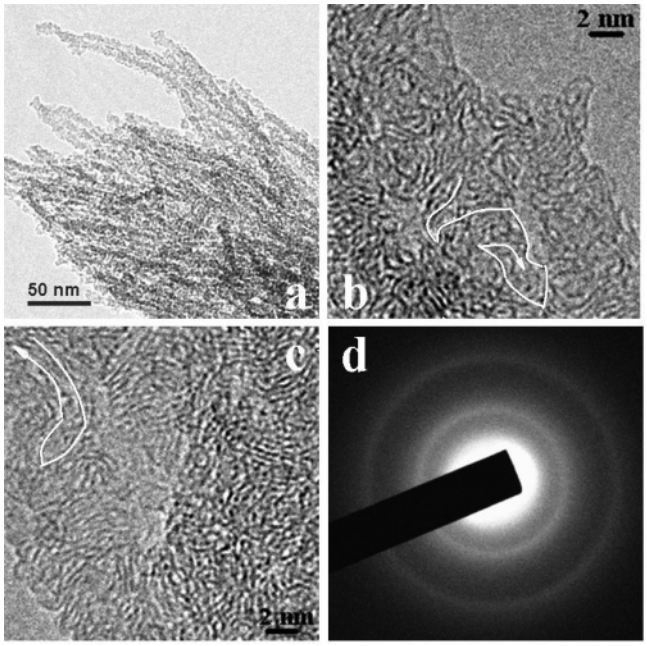

Figure 9. (a) TEM image, (b, c) HRTEM image, and (d) SAED pattern of the graphitized carbon nanofiber bundles prepared from the simple melt impregnation method by using Fe_2O_3 nanoparticle doped mesoporous silica as a template. The white arrows are observed spiral graphitized lattices.

carbons, suggesting a more graphitized carbon structure, which is due to the catalytic effect of the doping Fe_2O_3 nanoparticles during the carbonization process.[21]

TEM images of the graphitized carbon nanofiber bundles show a completely different graphitized structure compared with the mesoporous carbon products (Figure 9). Instead of ordered mesostructured carbon nanorod arrays, the bundles of carbon nanofibers are observed (Figure 9a), and the periodicity of the silica templates dramatically disappears. The diameters of the nanofibers are quite uniform because of the confinement effect of the silica templates, and the diameter of a single nanofiber is measured to be 7 nm, in good accord with the pore size of the silica templates.[17a] HRTEM images (Figure 9b,c) reveal that the graphitized structure is lacking the oriented periodicity like the hexagonal mesoporous carbon with graphitized structures mentioned above; however, a wormlike spiral graphitized structure has been observed (see the arrows in Figure 9b,c). Obviously, the crystallographic orientation of the graphic carbon is changed as the result of the growth of the graphite layers as we expected. The corresponding SAED pattern (Figure 9d) with a feature of polycrystalline materials also confirms the graphitized structure of the nanofiber bundles.

4. Electrochemical Property. The electrochemical property of the graphitized materials was studied by CV via a thin-film strategy. The amorphous mesoporous carbon, namely CMK-3, was also tested for comparison. CV curves are often employed to evaluate the potential possibility of the materials for being used for an electrochemical doubly-layered capacitor (EDLC) and the rectangle-shaped curves for charge/discharge process are considered to indicate the EDLC properties.[3] As Figure 10 shows, charge/discharge processes are clearly observed for the CV curves of the four samples recorded under the same condition. Comparably, the EDLC property of CMK-3 with an amorphous structure is the best among the samples, and the graphitized carbon nanofiber bundles yielded a similar curve. Although the latter sample is disordered nanofiber bundles, the spiral graphitized structure may be favored for the electrochemi-

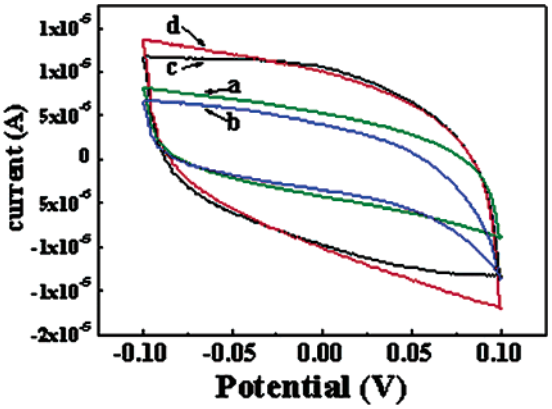

Figure 10. Cyclic voltammetry curves of ordered mesoporous graphitized carbon with (a) 2-D hexagonal *p6mm* and (b) bicontinuous cubic $Ia\bar{3}d$ symmetry, (c) graphitized carbon nanofiber bundles, and (d) mesoporous carbon CMK-3 prepared by using SBA-15 as a template and glucose as a carbon source.

SCHEME 2: Conductivity Profile of Graphitized Carbon along Different Crystallographic Planes

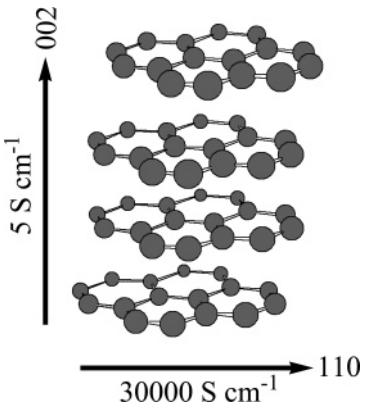

cal property judged from these experimental results. Interestingly, the EDLC property of the two types of ordered mesoporous carbons with ordered graphitized structure seems the worst. Part of the reason is the relatively small surface area of the two graphitized materials prepared from the simple melt impregnation, and the anisotropic graphite structure should be another important fact. Graphite is a kind of anisotropic solid and the conductivity of the material remarkably depends on the migration of the nonlocalized π electrons of the graphite layer. Therefore, as shown in Scheme 2, conductivity along the [002] direction, namely the growth direction of the mesopore walls of graphitc mesoporous carbon, is much lower than that along the [110] direction. When used as electrodes, the ion migration occurs in a direction of low conductivity of the graphitized mesoporous carbons, and the EDLC property is necessarily decreased. The spiral graphitized structure of the carbon nanofibers partly declines the anisotropic property of the materials and increases the conductivity along the ion migration direction, and that is why the EDLC property of the sample is better. When it comes to the two graphitized mesoporous carbon samples, the different mesostructure seems to have no influence on the EDLC properties. To fully understand the results, a more detailed study should be carried out for the actual graphitized orientation of the pore walls of the bicontinuous cubic mesoporous carbon.

Discussion

Compared with the previous reported preparation process of mesoporous carbons, the characteristic of our work is to employ a low-temperature melt impregnation procedure with mesophase pitches (MPs) as carbon precursors. The synthetic process can be elucidated based on the structural property of MPs (Scheme 3). The components of MPs are polyaromatic molecules and a single molecule is composed of several aromatic groups (molecular weight in the range of 800−1500) linked by short hydrocarbon chains such as $-CH_2-$.[12] With the strong $\pi-\pi$ stacking interaction of the large conjugated system, those planar polyaromatic molecules are assembled to small stacking units 2−3 nm in dimension. When melted above the softening temperature, the nonoriented stacking units will form quasi-aligned molecular units, which makes the materials more graphitizable.[12] Mesoporous silica used as the templates possesses abundant −OH groups and bridged O atoms (Si−O−Si) on the amorphous silica walls, and those groups play a very important role for the incorporation of MPs into the mesopores.

Speculating with the assistance of theoretical molecular simulation with the AM1 method, three types of noncovalent bond may possibly be formed between the Si−OH groups or bridged O atoms and MPs (the optimized molecular structure with lowest energy by AM1 computation[22] is shown in Scheme 3). First, there is an electrostatic interaction between the nonlocalized π electrons of the large conjugated system of MPs and the positive charged H atoms of Si−OH groups (the dihedral angle of the silica wall to the graphene layer is 58.2°). Due to the large volume of the molecular units of the MPs compared to the −OH groups, the noncovalent bonds are relatively difficult to form and will lead to a tilted fashion for stacking units of the MPs to enter the mesopores. In this way, the (002) plane of the graphite domains is not vertical to the channels of the templates, implying the defects formed occasionally. Second, another electrostatic interaction can also form with the negatively charged O atoms of −OH groups and the positive charged H atoms of the MPs (the dihedral angle of the silica wall to the graphene layer is 89.8°). Because of the volume matching of the two groups, this kind of noncovalent bond may be more predominate than the one mentioned above. Third, the positive charged H atoms of the MPs can also form noncovalent bonds with the bridged O atoms (the dihedral angle of the silica wall to the graphene layer is 89.9°). Due to the advantage of the interaction direction, these noncovalent bonds are dramatically easy to form. In Scheme 3, the later two interactions make the stacking units incorporate into the pores with the (002) plane vertical to the channels, and finally the oriented periodicity of the graphite domains comes into being. Capillary condensation is also important for the melt impregnation process, which causes the stacking units of MPs to go deeper inside the pores more easily. With the strong $\pi-\pi$ stacking interaction between the molecular units of MPs, the incorporating process remains in a persistent fashion and all these facts allow the mesopores of the templates to be completely filled with MPs. In the case of the bicontinuous cubic structure, the helical channels make the procedure much more complicated. But speculating based on the N_2 sorption and electrochemical results, a certain oriented periodicity still exists in the graphitized pore walls to make the carbon frameworks highly condensed and anisotropic.

As described above, the synthetic procedure artfully utilizes the noncovalent interaction of the chemical groups between the inorganic host and mesophase pitches. Fortunately, except for −OH groups, the bridged O atoms also participate in the assemblies to achieve the full incorporation of the MPs, which is quite beneficial to the whole procedure. As a result, other methods, such as microwave digestion or pore walls functionalization to enable better incorporation of precursors,[23−26] can

SCHEME 3: Mechanism of the Melt Impregnation Process for Preparing Ordered Mesoporous Carbon Materials with Ordered Graphite Structure[a]

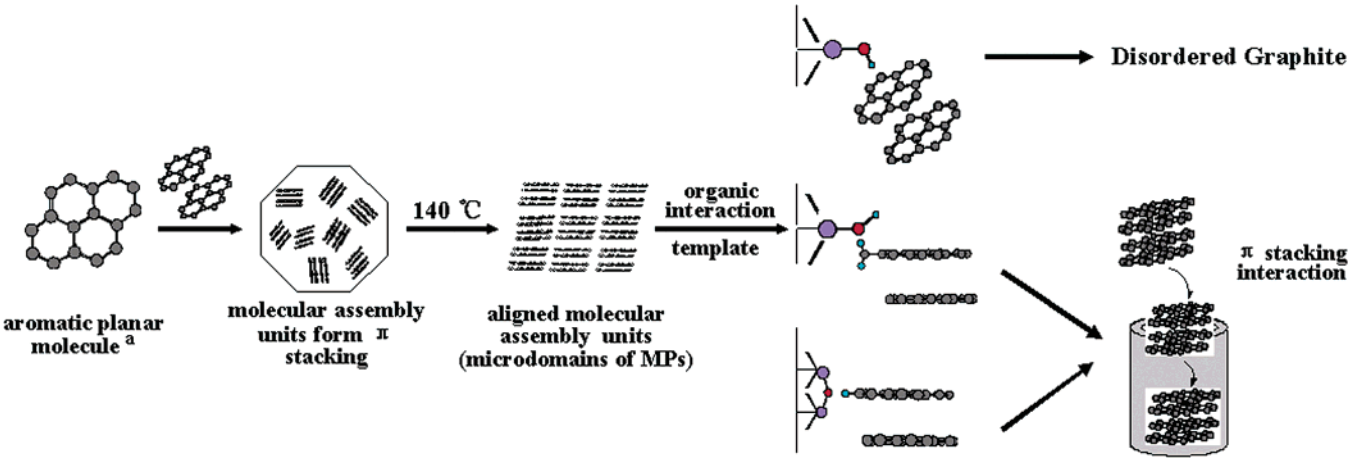

[a] MPs are constructed with polyaromatic molecules with molecular weight in the range of 800−1500, and the molecule in the scheme is just a symbol for polyaromatic compounds.

be avoided, and the preparation becomes more facile. Microwave digested SBA-15 with extremely abundant −OH groups[23] was also used as a template during the experiment. But no difference on mesostructure regularity and graphitized structure orientation was found based on XRD and TEM results, which verifies the above computation results.

To purposefully vary the orientation of the graphitized layers, Fe_2O_3 nanoparticle doped mesoporous silica was used as a template. Fe_2O_3 is an excellent catalyst for the graphitization process of the carbon materials and the metal oxide can remarkably decrease the growth temperature of the polyaromatic layer to produce more graphitized carbon.[20] In our experiments, after incorporation of mesophase pitches, the nanoparticles are highly dispersed in the carbon matrix. Therefore, it is not difficult to understand that the graphite layers may grow larger than normal samples at the same calcination temperature. With the confinement effect of the mesopores, the large graphitized layers curl inside the pores and form a spiral structure.

Different experimental conditions are tested to optimize the impregnation method for more ordered and graphitized mesoporous carbons. There are two main points that impact the synthetic procedure. First, the quantity of the MPs should be a key point for the successful synthesis. For MPs, during the heating carbonization at about 400−500 °C, the small hydrocarbon species pyrolyze and give outgases, which makes the volume of MPs swell a lot[12] and forms outside carbon coverage to weaken the structural regularity. Therefore, the amount of MPs (calculated from its density and the pore volume of the template) should be decreased about 20% for the consideration of the swelling effect, and the carbon coverage at the outer surface can be avoided. Second, the impregnation temperature should be well-selected. As we discussed above, the capillary condensation significantly affects the incorporation, which is closely related to the viscosity of MPs. Above the softening temperature, the viscosity of MPs becomes smaller and smaller as the temperature increases, and finding a proper temperature point is very important. In our synthesis, the softening temperature of the MPs is 104 °C, and the impregnation temperature is 140 °C.

Conclusions

We have demonstrated a simple melt impregnation method to prepare ordered mesoporous carbons with graphite structure at low temperature by using MPs as the carbon precursor. A facile one-step melt impregnation procedure is simply impregnating the MP melt into the channels of mesoporous silica templates. Two types of ordered mesoporous graphitized carbon materials and graphitized carbon nanofiber bundles have been successfully obtained. The walls of the hexagonal mesoporous carbons are composed of graphitized domains with the (002) crystallographic plane of the graphite perpendicular to the *c* axis of the mesostructure. Theoretical computations reveal that the interaction of the bridged O atoms of the silica walls with the H atoms of the MPs contributes to this orientation. Ordered bicontinuous cubic mesoporous carbons are true replica frameworks of $Ia\bar{3}d$ symmetry. Graphitized carbon nanofiber bundles with a uniform diameter of about 7 nm show a spiral graphite structure with excellent electrochemical charge/discharge processes. The method can be widely applied to the hard-templating synthesis of graphite nanostructures and other doped carbon nanomaterials.

Acknowledgment. We thank Y. Chen for TEM measurements, and we gratefully acknowledge the support of this research by the NSFC (20173012, 20233030, 20373013, 20101002), State Key Basic Research Program of PRC (2001CB610505, 2002AA321010), Shanghai Nanotechnology Center (0212nm043), and Fudan Graduate Innovation Funds.

References and Notes

(1) (a) Ryoo, R.; Joo, S. H.; Jun, S. J. *J. Phys. Chem. B* **1999**, *103*, 7743. (b) Lee, J.; Yoon, S.; Hyeon, T.; Oh, S. M.; Kim, K. B. *Chem. Commun.* **1999**, *21*, 2177.

(2) Ryoo, R.; Joo, S. H.; Kruk, M.; Jaroniec, M. *Adv. Mater.* **2001**, *13*, 677.

(3) Yoon, S.; Lee, J.; Hyeon, T.; Oh, S. M. *J. Electrochem. Soc.* **2000**, *147*, 2507.

(4) Yang, H.; Shi, Q.; Liu, X.; Xie, S.; Jiang, D.; Zhang, F.; Yu, C.; Tu, B.; Zhao, D. *Chem. Commun.* **2002**, *23*, 2842.

(5) Joo, S. H.; Choi, S.; Oh, J. I.; Kwak, J.; Liu, Z.; Terasaki, O.; Ryoo, R. *Nature* **2001**, *412*, 169.

(6) Che, S.; Garcia-Bennett, A. E.; Liu, X.; Hodgkins, R. P.; Wright, P. A.; Zhao, D.; Terasaki, O.; Tatsumi, T. *Angew. Chem., Int. Ed.* **2003**, *42*, 3930.

(7) Kruk, M.; Jaroniec, M.; Kim, T. W.; Ryoo, R. *Chem. Mater.* **2003**, *15*, 2815.

(8) Kaneda, M.; Tsubakiyama, T.; Carlsson, A.; Sakamoto, Y.; Ohsuna, T.; Terasaki, O.; Joo, S.; Ryoo, R. *J. Phys. Chem. B* **2002**, *106*, 1256.

(9) Darmstadt, H.; Roy, C.; Kaliaguine, S.; Joo, S. H.; Ryoo, R. *Micorporous Mesoporous Mater.* **2003**, *60*, 139.

(10) Darmstadt, H.; Roy, C.; Kaliaguine, S.; Choi, S. J.; Ryoo, R. *Carbon* **2002**, *40*, 2673.

(11) Kim, T. W.; Park, I. S.; Ryoo, R. *Angew. Chem., Int. Ed.* **2003**, *42*, 4375.

(12) Mochida, I.; Korai, Y.; Ku, C. H.; Watanabe, F.; Sakai, Y. *Carbon* **2000**, *38*, 305.

(13) Dumont, M.; Chollon, G.; Dourges, M. A.; Pailler, R.; Bourrat, X.; Naslain, R.; Bruneel, J. L.; Couzi, M. *Carbon* **2002**, *40*, 1475.

(14) Li, Z.; Jaroniec, M. *J. Am. Chem. Soc.* **2001**, *123*, 9208.

(15) (a) Vix-Guterl, C.; Saadallah, S.; Vidal, L.; Reda, M.; Parmentier, J.; Patarin, J. *J. Mater. Chem.* **2003**, *13*, 2535. (b) Li, Z.; Jaroniec, M. *J. Phys. Chem. B* **2004**, *108*, 824. (c) Yang, N.; Jian, K.; Kulaots, I.; Crawford, G.; Hurt, R. *J. Nanosci. Nanotechnol*. **2003**, *3*, 386.

(16) Zhao, D.; Feng, J.; Huo, Q.; Melosh, N.; Fredrickson, G. H.; Chmelka, B. F.; Stucky, G. D. *Science* **1998**, *279*, 548.

(17) Kleitz, F.; Choi, S.; Ryoo, R. *Chem. Commun*. **2003**, *17*, 2136.

(18) (a)Yang, H.; Shi, Q.; Tian, B.; Lu, Q.; Gao, F.; Xie, S.; Fan, J.; Yu, C.; Tu, B.; Zhao, D. *J. Am. Chem. Soc.* **2003**, *125*, 4724. (b) Yang, H.; Shi, Q.; Tian, B.; Xie, S.; Zhang, F.; Yan, Y.; Tu, B.; Zhao, D. *Chem. Mater*. **2003**, *15*, 536. (c) Melosh, N.; Davidson, P.; Chmelka, B. F. *J. Am. Chem. Soc*. **2000**, *122*, 823.

(19) Jun, S.; Joo, S. H.; Ryoo, R.; Kruk, M.; Jaroniec, M.; Liu, Z.; Ohsuna, T.; Terasaki, O. *J. Am. Chem. Soc*. **2000**, *122*, 10712.

(20) Kruk, M.; Jaroniec, M.; Ryoo, R.; Joo, S. *J. Phys. Chem. B* **2000**, *104*, 7960.

(21) Wang, Y.; Korai, Y.; Mochida, I.; Nagayama, K.; Hatano, H.; Fukuda, N. *Carbon* **2001**, *39*, 1627.

(22) Frisch, M. J.; Trucks, G. W.; Schlegel, H. B.; Scuseria, G. E.; Robb, M. A.; Cheeseman, J. R.; Zakrzewski, V. G.; Montgomery, J. A., Jr.; Stratmann, R. E.; Burant, J. C.; Dapprich, S.; Millam, J. M.; Daniels, A. D.; Kudin, K. N.; Strain, M. C.; Farkas, O.; Tomasi, J.; Barone, V.; Cossi, M.; Cammi, R.; Mennucci, B.; Pomelli, C.; Adamo, C.; Clifford, S.; Ochterski, J.; Petersson, G. A.; Ayala, P. Y.; Cui, Q.; Morokuma, K.; Malick, D. K.; Rabuck, A. D.; Raghavachari, K.; Foresman, J. B.; Cioslowski, J.; Ortiz, J. V.; Stefanov, B. B.; Liu, G.; Liashenko, A.; Piskorz, P.; Komaromi, I.; Gomperts, R.; Martin, R. L.; Fox, D. J.; Keith, T.; Al-Laham, M. A.; Peng, C. Y.; Nanayakkara, A.; Gonzalez, C.; Challacombe, M.; Gill, P. M. W.; Johnson, B. G.; Chen, W.; Wong, M. W.; Andres, J. L.; Head-Gordon, M.; Replogle, E. S.; Pople, J. A. *Gaussian 98*, Revision A.1; Gaussian, Inc.: Pittsburgh, PA, 1998.

(23) (a) Tian, B.; Liu, X.; Yang, H.; Xie, S.; Yu, C.; Tu, B.; Zhao, D. *Adv. Mater*. **2003**, *15*, 1370. (b) Tian, B.; Liu, X.; Solovyov, L. A.; Liu, Z.; Yang, H.; Zhang, Z.; Xie, S.; Zhang, F.; Tu, B.; Yu, C.; Terasaki, O.; Zhao, D. *J. Am. Chem. Soc.* **2004**, *126*, 865.

(24) Lin, H.; Mou C. *Acc. Chem. Res*. **2002**, *35*, 927.

(25) Lee, C.; Lin, T.; Mou, C. *J. Phys. Chem. B* **2003**, *107*, 2543.

(26) Lee, C.; Lin, T.; Lin, H.; Zhao, Q.; Liu, S.; Mou, C. *Micorporous Mesoporous Mater*. **2003**, *57*, 199.